



# Synthesis and characterization of hybrid conducting composites based on polyaniline/magnetite fillers with improved microwave absorption properties

Belkacem Belaabed<sup>a,\*</sup>, Jean Luc Wojkiewicz<sup>b,c</sup>, Saad Lamouri<sup>a</sup>, Nouredine El Kamchi<sup>b,c</sup>, Tuami Lasri<sup>b</sup>

<sup>a</sup> Laboratoire de Chimie Macromoléculaire, Ecole Militaire Polytechnique (EMP), Bordj El Bahri, 16111 Alger, Algeria

<sup>b</sup> Univ. Lille Nord de France, F-59000 Lille, France

<sup>c</sup> Ecole des Mines de Douai, CE, F-59508 Douai, France

## ARTICLE INFO

### Article history:

Received 31 January 2012

Received in revised form 22 February 2012

Accepted 26 February 2012

Available online xxx

### Keywords:

Polyaniline

Magnetite

Epoxy resin composites

Complex permittivity

Magnetic permeability

Electromagnetic absorbers

## ABSTRACT

Hybrid organic/inorganic electromagnetic absorbing materials (EMAMs) based on polyaniline (PANI) and magnetite ( $\text{Fe}_3\text{O}_4$ ) fillers dispersed in epoxy resin matrix were successfully prepared for electromagnetic applications. The effects of PANI and  $\text{Fe}_3\text{O}_4$  loading on permittivity, permeability and microwave absorption properties were studied. The structure and the morphology of the elaborated composites were investigated by X-ray diffraction (XRD) and scanning electron microscopy (SEM). Electromagnetic properties and absorbing behaviors were performed over frequency range of 12.4–18 GHz (Ku-band). The results show that synthesis parameters such as amount and particle size of PANI and used  $\text{Fe}_3\text{O}_4$  affect significantly the morphology, the conductivity, and the microwave absorption properties of the final materials. It was revealed that the electromagnetic parameters were higher in hybrid PANI/magnetite/epoxy resin than in dielectric PANI/epoxy resin composites. The permittivity and the permeability parameters increased to high values with the rate of fillers in the composite and remained constant with the frequency. A minimum reflection coefficient (RC) of  $-42$  dB was observed at 16.3 GHz with a thickness around 1 mm for composites containing 15% of PANI and 10% of  $\text{Fe}_3\text{O}_4$  ( $\epsilon' = 10$ ) and  $-37.4$  dB at 14.85 GHz for the composite of 15% of PANI and 25% of  $\text{Fe}_3\text{O}_4$  ( $\epsilon' = 17$ ). However, a composite made with only 20% of PANI ( $\epsilon' = 8.5$ ) showed a minimum reflection coefficient of  $-11$  dB at 18 GHz with the same thickness. The possibility to modulate the electromagnetic properties of the composite materials is of a great interest to fabricate microwave absorbing and electromagnetic shielding materials with high performances.

© 2012 Elsevier B.V. All rights reserved.

## 1. Introduction

The high proliferation of electronic instruments especially in the telecommunication area causes electromagnetic interferences (EMI) and disturbs the effective performance of electronic or electrical circuits in military and civil uses [1,2]. To assure the safety operation of electronic devices, standard rules are imposed to the designers of electronic equipments to protect those against the aggression of electromagnetic waves. Then, the designers have to conceive enclosures to limit the coupling between the electromagnetic field and the electronic circuits. In regard to the application, these enclosures have to reflect or absorb the electromagnetic waves. In stealth weapon defense system, advanced composite materials are used as electromagnetic absorbing materials (EMAMs) to attenuate the electromagnetic beam and reduce the radar cross section (RCS) [3,4]. Thus, several needs to develop thinner and lighter electromagnetic wave absorbers with wider

absorbing band-widths are continuously increasing. Electromagnetic absorbing materials (EMAMs) may be classified as magnetic or dielectric. Actually, these materials have attracted a great attention due to their improved microwave absorption properties, which are relevant to multiform electromagnetic losses based on magnetic and dielectric loss [5]. Dielectric and magnetic EMAMs interact in different ways with the electromagnetic radiation but the final result of these interactions is the same in the sense that the energy of the incident wave is transformed into heat [6]. Usually, these materials are obtained by the dispersion of one or more types of absorbing fillers in a matrix. They can be produced in different forms such as paints, sheets, and thin films as single, double or multi-layer [7]. In each application, it is necessary to control precisely the physical properties of the material in terms of permittivity, magnetic permeability and conductivity and to know their variations with the frequency [8]. This can be achieved by the use of suitable fillers such as aluminum, carbon, graphite, aluminum nitrides, nickel, zinc sulfide, titanium dioxide, silver particles or barium titanate [9–12]. But the mechanical properties of the materials are deteriorated with the rate of loading and the weight of the material becomes incompatible with the aeronautical

\* Corresponding author. Tel.: +213 661 169 752; fax: +213 218 632 04.  
E-mail address: [belaabed@yahoo.fr](mailto:belaabed@yahoo.fr) (B. Belaabed).

applications. For those reasons, intrinsically conducting polymers and particularly, polyaniline became a credible alternative. They show a good thermal and chemical stability, an easy tunability of their electronic properties and high levels of electromagnetic shielding performances at microwave frequencies with a low mass by unit of surface [13–16]. The electromagnetic properties of polyaniline can be modified by the addition of inorganic fillers. The inclusion of magnetic particles may improve the magnetic and dielectric properties of host materials. Therefore, polyaniline combined with magnetic particles provides materials exhibiting novel functionalities [17]. Magnetite ( $\text{Fe}_3\text{O}_4$ ) is a subject of scientific and technological interest, due to its good magnetic and electrical properties and a very high saturation magnetization. Consequently, by incorporation of dielectric and magnetic fillers, the electromagnetic properties of such materials can be improved to obtain a maximum absorption of electromagnetic energy. Over the last decade, many researches focused on a new type of hybrid material based on polymers-matrix composites containing dielectric or/and magnetic fillers [18]. Combination of PANI with other organic or inorganic materials provides new materials with tailored properties, suitable for various electrical and electromagnetic applications in aeronautic or aerospace areas and to avoid electromagnetic pollution arising from various electronic devices operating in microwave frequency range [19,20]. The dispersion of polyaniline and magnetite fillers in an insulating polymer matrix (thermoplastic or thermosetting) produces different composites that can absorb and reflect electromagnetic radiation by changing its conductivity, its dielectric constant and its magnetic permeability. Epoxy resins cured by anhydride agent are widely used as coatings, adhesives and insulators in the industry due to their good mechanical properties, including a high modulus, good electrical and thermomechanical properties, and excellent cohesiveness compared to many other materials [21,22]. New materials such as electromagnetic wave absorbing material composites can be developed by combining the good mechanical properties of epoxy resin with the high performance of electrical and magnetic properties of PANI and  $\text{Fe}_3\text{O}_4$  [23]. The absorption loss is proportional to the shield thickness and is a function of the conductivity, the permittivity and the permeability [24,25]. Furthermore, in advanced applications, small thickness, wide band absorptions, light weight, high strength and high absorbing property are used to appraise the absorbing performance [26,27].

The aim of the present study is the synthesis and the characterization of hybrid microwave absorbers. Thus, epoxy resin composites with anhydride as a hardener were prepared with different amounts of PANI and  $\text{Fe}_3\text{O}_4$  fillers. The structure and the morphology of the samples were investigated by X-ray diffraction (XRD) and scanning electron microscopy (SEM). The influence of the filler content with respect to the electromagnetic properties of composites has been investigated. Complex permittivity and permeability and microwave absorption property of the composites with different thickness were studied in the Ku band (12.4–18 GHz) using microwaves guides and a Vector Network Analyzer (VNA).

## 2. Experimental

### 2.1. Materials

Commercial medapoxy inject (ER) was obtained from Algerian Granitex. Tetrahydrofuran (THF), magnetite ( $\text{Fe}_3\text{O}_4$ ) 99.9% of purity, boron trifluoride ethylamine complex ( $\text{BF}_3$ -complex 95% of purity), hexahydrophthalic anhydride (HHPA) and polyaniline doped para-toluene sulfonic acid (PANI-PTSA) with conductivity value of 400–600 S/m and 2–3  $\mu\text{m}$  of particle size were purchased from Sigma-Aldrich.

### 2.2. Composite preparation

Composites of PANI/epoxy resin and hybrid PANI/ $\text{Fe}_3\text{O}_4$ /epoxy resin, cured by HHPA/ $\text{BF}_3$ -complex were prepared by mixing process. PANI and  $\text{Fe}_3\text{O}_4$  were

dispersed in THF as solvent separately for 1 h then, the two dispersions were mixed using an ultrasonic bath for 3 h at 50 °C, followed by mechanical stirring to improve the dispersion quality and to avoid aggregates. Then, epoxy resin was added to the above mentioned solution at a continuous moderate mechanical stirring speed and heating temperature of 65 °C for 4 h to remove the solvent residues that have an evaporation point below the crosslinking temperature and to assure high dispersion quality and a homogeneous mixture [28]. The weight contents of the PANI and magnetite in the composites varied from 1 to 25 wt%. When the solvent is evaporated, 81.5 parts of the curing agent with catalyst was added for 100 parts of epoxy resin [29]. The obtained mixture was immediately poured into appropriate molds to provide films with different thicknesses. The films were subjected to crosslinking steps in a thermostatic oven vacuum, first baking at 80 °C for 4 h and then post-curing at 120 °C for 24 h. In the same manner, composites of PANI (15%) with magnetite loading from 5 to 25% were prepared.

### 2.3. Instrumental analysis

XRD analysis of the samples were performed at room temperature using a D8 Advance-Bruker AXS diffractometer with  $\text{CoK}\alpha$  radiation at a wavelength of 1.78897 Å, operating at 40 kV and 35 mA in the range of  $2\theta = 10$ –80°. Morphological analyses were carried out with a scanning electron microscope type Hitachi S-4300 SE/N operating between 5 kV and 20 kV and 35–50  $\mu\text{A}$ . In order to avoid the effect of electric charge on the surface and to facilitate the flow of the electrons, the samples were coated with a thin layer of gold. The electrical conductivity of the different samples was measured at room temperature with a four-probe method. Pellets with a thickness of 0.5–0.6 mm of filler powder were prepared, and thin contact points of gold were deposited to ensure good contact between the sample and the electrode. The DC conductivity was calculated from the current–voltage dependence. Electromagnetic reflected and transmitted scattering parameters ( $S_{11}$ ,  $S_{21}$ ), were carried out performing wave guide measurements between 12.4 and 18 GHz in transmission and reflection mode using WR-62 wave-guide for the Ku band and a Vector Network Analyzer (VNA) type Agilent technologies, E8362B working from 10 MHz to 20 GHz. Samples were prepared and cured into rectangular holder with different thicknesses and clamped between two flanges of the input and output wave guides. The wave-guides were connected to the vectorial network analyzer with two cables in APC7 standards. To measure the reflection coefficient  $S_{11}$  and transmission coefficient  $S_{21}$ , custom designed TRL calibration kits are applied [30]. Great attention was brought to avoid air gap between the sample and the wave

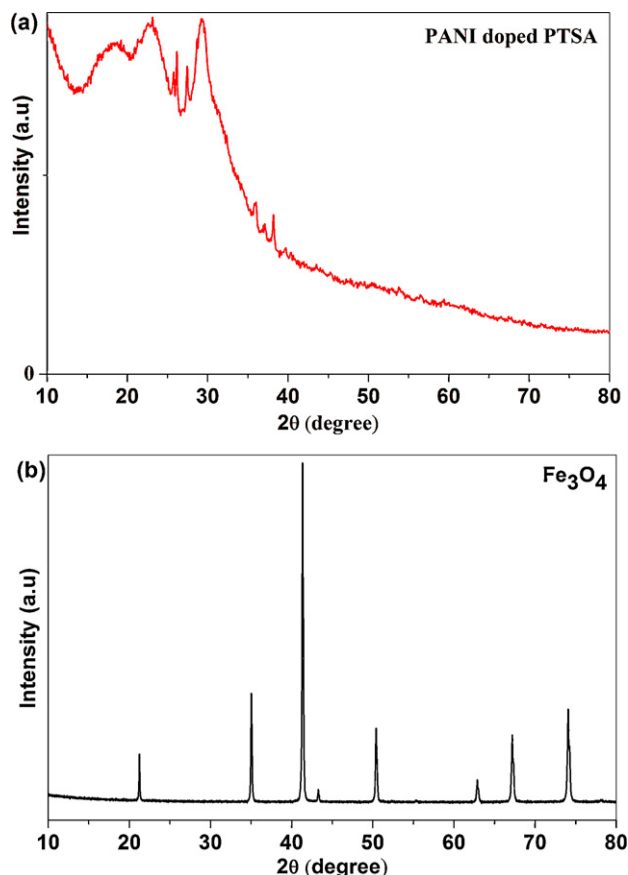


Fig. 1. X-ray diffraction plots of PANI-PTSA (a) and  $\text{Fe}_3\text{O}_4$  powder (b).

guide. The Nicolson–Ross–Weir model [31] was used to extract the real and imaginary parts of the complex permittivity ( $\epsilon^*$ ) and the complex permeability ( $\mu^*$ ) from the measured values of ( $S_{11}$  and  $S_{21}$ ). Microwave absorption properties were measured using the same instrument but the rear face of the sample was terminated by a short-circuit that is a perfect conductor. All measurements were repeated several times to ensure the repeatability of data.

### 3. Results and discussion

#### 3.1. Structure and morphology study

X-ray diffraction was used to further probe the phase identification and crystalline structures of the samples. X-ray diffraction patterns of the PANI and  $\text{Fe}_3\text{O}_4$  are presented in Fig. 1.

It is well known that crystalline or semi-crystalline polymers are two-phase systems containing ordered and disordered regions. Doped polyaniline is a heterogeneous system consisting of a partially crystalline regions and amorphous regions [32]. In our case, PANI-doped PTSA presents a signal that exhibits a main reflections located at  $2\theta = 18.5^\circ$ ,  $23^\circ$  and a strong peak at  $2\theta = 29.5^\circ$  which may be ascribed to the periodicity parallel and periodicity perpendicular to the polymer chain respectively. However the polyaniline

emeraldine base (PANI-EB) powder exhibits a broadened pattern, indicating its amorphous structure [33–36]. In PANI-PTSA, the sharpness of the peaks represents the degree of orientation of the polymer chains in that particular crystal plane, and the intensity represents the population of crystallites in that plane. These results are in concordance with SEM observations and are in agreement with those of the literature [37–40]. Thus, our results indicate an orthorhombic structure of the crystalline phases of PANI.

The main characteristic peaks of the X-ray patterns (Fig. 1b) of the distinctive  $\text{Fe}_3\text{O}_4$  nanoparticles located at  $2\theta = 21.23^\circ$ ,  $35^\circ$ ,  $41.35^\circ$ ,  $43.3^\circ$ ,  $50.4^\circ$ ,  $67.18^\circ$  and  $74^\circ$ , identify the face-center cubic phase with no impurity peak and the high crystalline structure of the magnetite which characterized by the strong and sharp peak at  $2\theta = 41.35^\circ$ . These results are in agreement with those reported in the literature [41–43]. All of the composite samples with different ratios of fillers exhibit broad signal patterns. This broad X-ray structure suggests an amorphous character of the prepared composites.

The morphology of the PANI, magnetite and their composites was investigated using a scanning electron microscope (SEM). The micrographs were obtained on metalized films deposited on a silicon sheet and the results are shown in Fig. 2.

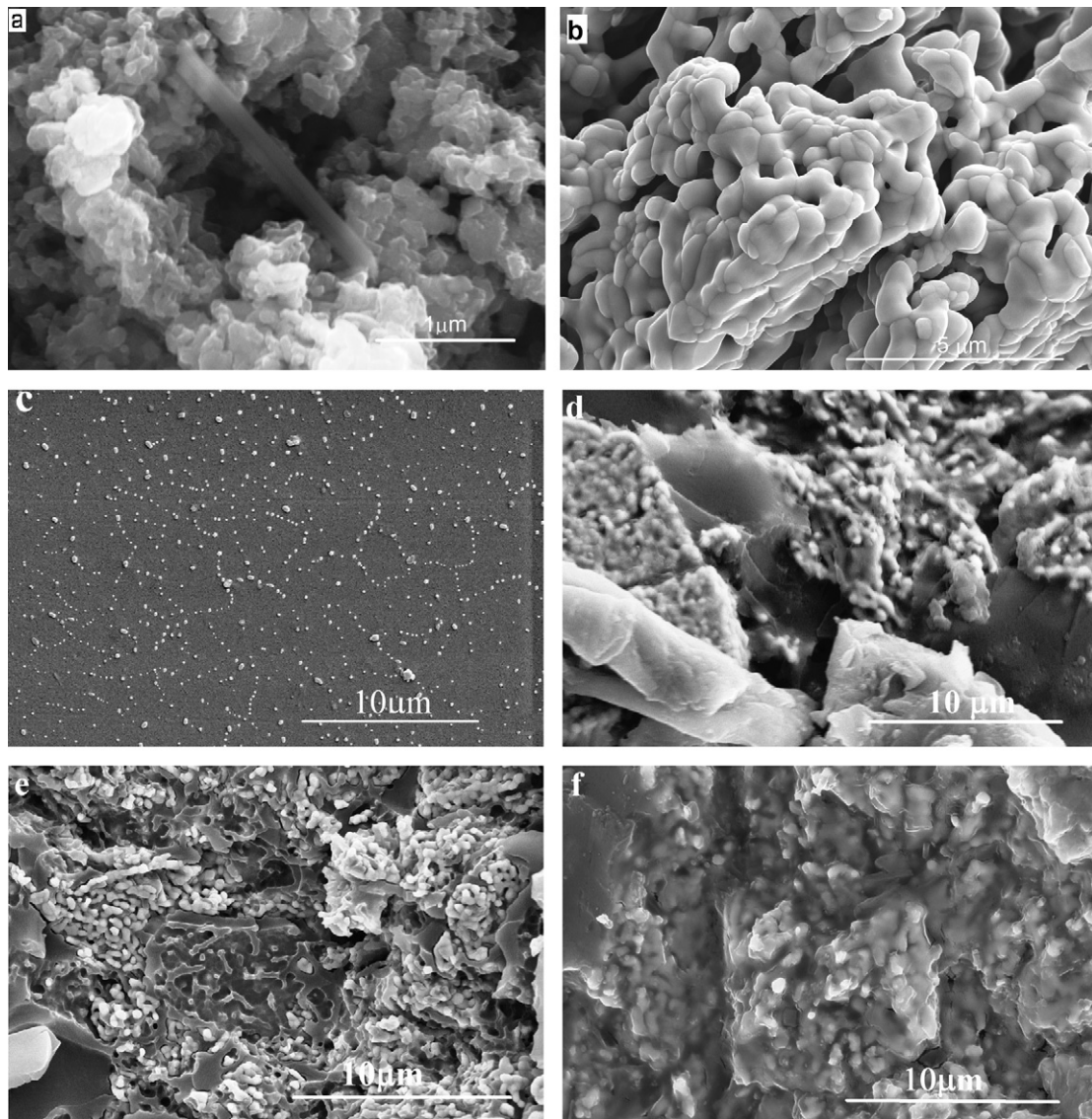


**Fig. 2.** SEM micrographs of PANI-PTSA powders (a),  $\text{Fe}_3\text{O}_4$  powders (b), PANI-PTSA (15%) (c), and hybrid composite of: PANI (15%)/ $\text{Fe}_3\text{O}_4$  (10%) (d), PANI (15%)/ $\text{Fe}_3\text{O}_4$  (15%) (e), and PANI (15%)/ $\text{Fe}_3\text{O}_4$  (20%) (f).



In these images, we note in the case of PANI (Fig. 2a), the existence of lamellar, linear in approximately 1–2  $\mu\text{m}$  in size and a crystalline form in size below 0.5  $\mu\text{m}$ , with flat and smooth surfaces, although the latter is the dominant morphology in the PANI micrographs, this confirms that the doping agent used gives a pseudo-metallic characteristic of PANI. In magnetite micrograph, we observe a crystalline morphology with micro porous structure which has seldom been reported in the literature. This structure is correlated with X-ray investigation. In the SEM micrographs of cured composites films, the white regions are the filler particles. For low ratios of fillers, the PANI and magnetite particles are homogeneously and randomly dispersed in the epoxy matrix, indicating a homogeneous mixture of phases and good compatibility. It is believed that PANI and  $\text{Fe}_3\text{O}_4$  fillers are well dispersed in epoxy resin composites because of the use of the vigorous stirring procedure based on magnetic stirring, mechanical and sonication for long time before curing process. Moreover polyaniline penetrates in porous regions of magnetite, and makes the contact between particle fillers. When the fillers, with their electrical conductivity characteristics are anchored in a support, they form electrical conduction paths, which favor the Ohmic loss of incident energy. However, when the weight content of fillers in the samples is above 15 wt.%, agglomerates of fillers are formed in the matrix

### 3.2. Electrical and microwave study

The complex permittivity ( $\varepsilon^* = \varepsilon' - i\varepsilon''$ ) and the complex permeability ( $\mu^* = \mu' - i\mu''$ ) can be derived from the measured reflected and transmitted scattering parameters ( $S_{11}$  and  $S_{21}$ ), determined directly by the VNA and using the Nicholson–Ross and Weir method [30,44].

As we know, real ( $\varepsilon'$ ,  $\mu'$ ) and imaginary ( $\varepsilon''$ ,  $\mu''$ ) parts of complex permittivity and permeability characterize the storage ability and

the loss of electric and magnetic energy respectively of materials [45,46].

The electrical conductivity of the PANI doped PTSA was measured at room temperature using a four-probe technique. The DC conductivity of the composite containing more than 15% (wt.%) of fillers is on the order of 0.1–10 S/m. The conductivity of the composites increases with the content of fillers.

The frequency dependence in the range 12.4 to 18 GHz of the complex permittivity ( $\varepsilon'$ ,  $\varepsilon''$ ), the complex permeability ( $\mu'$ ,  $\mu''$ ),  $\tan(\delta)$  and the conductivity of polyaniline/epoxy resin and polyaniline/magnetite/epoxy resin hybrid composites with 15% of PANI and different contents of magnetite were investigated below.

#### 3.2.1. PANI–epoxy resin composites

Fig. 3 shows the real and imaginary parts, the  $\tan(\delta)_\varepsilon$  and the conductivity of the PANI/epoxy resin composites. It can be seen that the values of the dielectric constant do not significantly vary with increasing frequency.

For the imaginary part  $\varepsilon''$ , the values show insignificant variation at frequency ranging from 12.4 to 18 GHz. It is found that, the values of the real and imaginary parts are jumped from 3.12 and 0.15 to 8.45 and 1.2 respectively when the PANI content in composites increases from 1 to 20%. A value of 0.02 and 0.16 of  $\tan(\delta)_\varepsilon$  was reached

#### 3.2.2. PANI– $\text{Fe}_3\text{O}_4$ /epoxy resin hybrid composites

It is observed in Fig. 4, that in all samples based on hybrid PANI/magnetite/epoxy resin composites, the real part ( $\varepsilon'$ ) and imaginary part ( $\varepsilon''$ ) of permittivity are higher than that of PANI/epoxy resin composites. In the whole frequency range and for all specimens, the real and imaginary parts of permittivity and permeability increase with fillers loading. Furthermore, the  $\varepsilon'$ ,  $\mu'$ ,  $\mu''$  and the  $\tan(\delta)_\mu$  decrease slightly with increasing frequency, however,  $\varepsilon''$  and  $\tan(\delta)_\varepsilon$  increase with frequency. A minimum and a

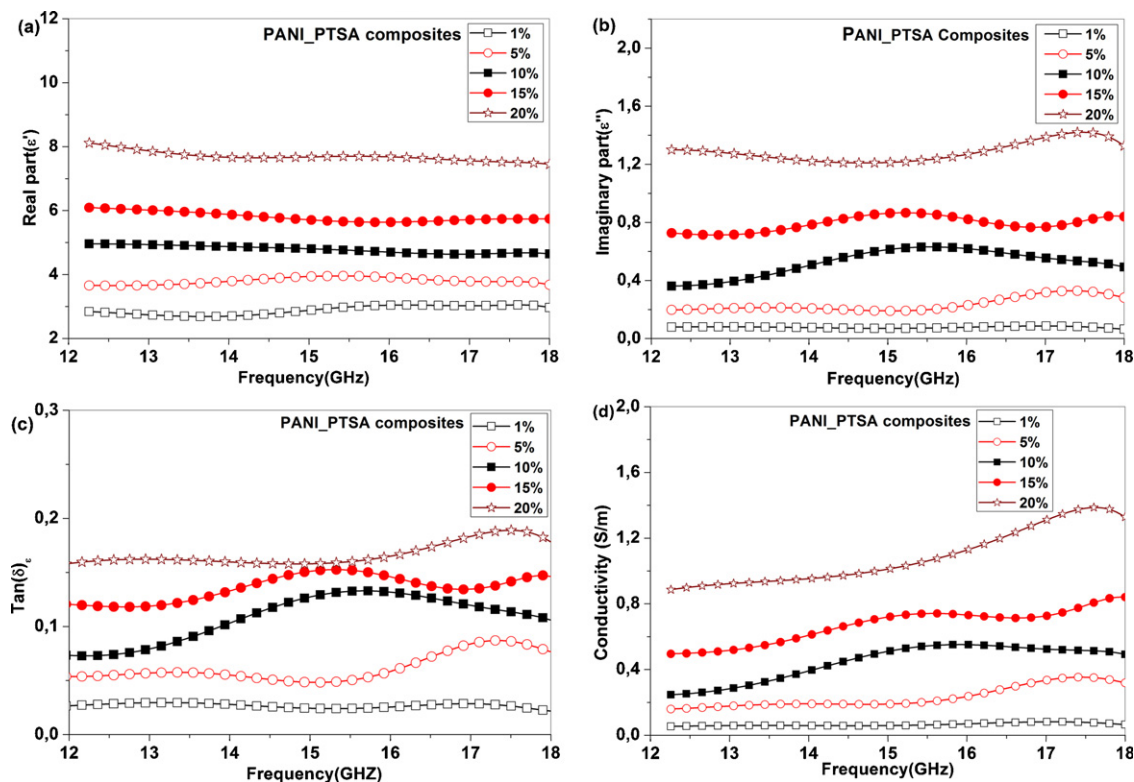
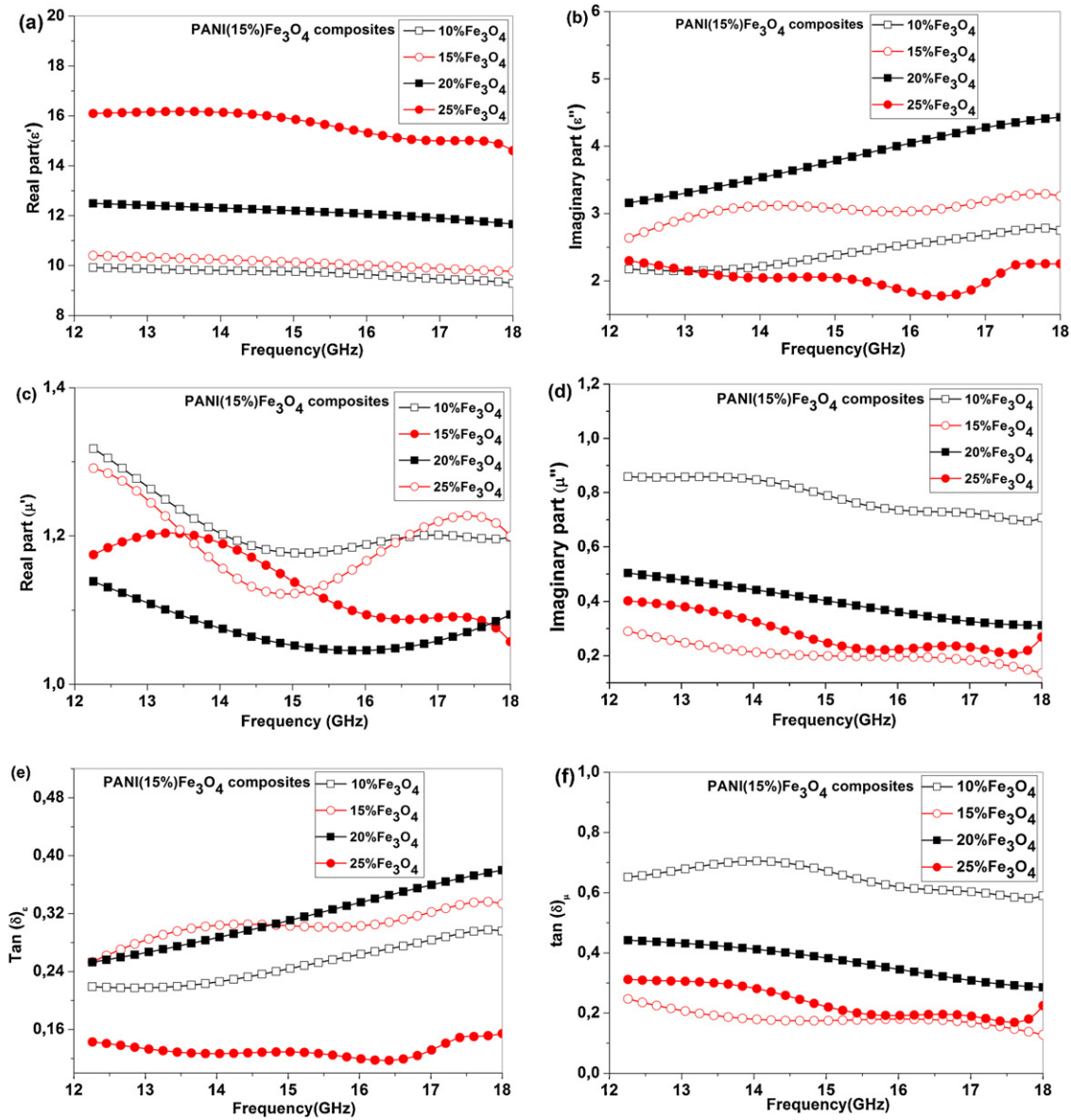


Fig. 3. The PANI/epoxy resin composites frequency dependence of real part of complex permittivity (a), imaginary part of complex permittivity (b),  $\tan(\delta)$  (c) and the conductivity (d).



**Fig. 4.** The PANI-PTSA (15%)/Fe<sub>3</sub>O<sub>4</sub>/epoxy resin hybrid composites frequency dependence of: real part of complex permittivity (a), imaginary part of complex permittivity (b),  $\tan(\delta)_\epsilon$  (c), real part of complex permeability (d), imaginary part of complex permeability (e) and  $\tan(\delta)_\mu$  (f).

maximum values of (10.5 and 2) and (17 and 2.5) of the  $\epsilon'$  and  $\epsilon''$  are obtained respectively at 10 and 25% of magnetite at the same content of 15% of PANI. Moreover, the real ( $\mu'$ ) and imaginary ( $\mu''$ ) parts of the permeability are 1.4 and 1.2 which decrease with increasing frequency as it can be seen in Fig. 4e and f. These values lead to a dielectric loss  $\tan(\delta)_\epsilon$  of 0.1 and a magnetic loss  $\tan(\delta)_\mu$  of 0.45 at higher content of magnetite, which decreases with frequency increase.

It was reported that, in polyaniline strong polarization occurs due to the presence of polaron/bipolaron, which leads to high value of  $\epsilon'$  and  $\epsilon''$ . With the addition of Fe<sub>3</sub>O<sub>4</sub> to polyaniline in the matrix, a significant increase in real and imaginary part of complex permittivity was observed [47].

The increase of the filler content results in a smaller distance between inclusions, leading to a larger capacitance of the system that is somehow included in the real part of permittivity term. It is believed that the accumulation of charges at the interface between the filler particles and the epoxy resin results in a large-scale field distortion. Thus the higher permittivity level can be attributed to

the increase of fillers in epoxy resin matrix [45,48,49]. The addition of PANI with Fe<sub>3</sub>O<sub>4</sub> in the matrix and the elimination of agglomerates surrounded by an insulating matrix results in the formation of a fine network, which allows charge transfer to occur easily through the well-ordered polymer, leading to enhanced dielectric properties of the composites. An increase of the charges (PANI and Fe<sub>3</sub>O<sub>4</sub>) content in the composites increases the dipole density by ordering the arrangement of chains in the disordered polymer. With the application of an external electric field, strong dipole-dipole interactions between the fillers and epoxy resin allow the charges to hop from one dipole to another throughout the polymer composite matrix. As the amount of the charges increases, the dipole density increases with the mobility of the dipoles, this in turn depends upon the mobility of the polymer chains to which the dipoles are attached [45,50]. As a result, an increase in the values of the permittivity and dielectric loss factor are observed with increasing fillers in the composites [51]. These results reveal that the addition of PANI and magnetite fillers in matrix increases the dielectric and magnetic loss of composites which enhance the electromagnetic

properties and make it interesting for electromagnetic absorbing applications [52–56].

### 3.3. Microwave absorbing properties

According to the transmission line theory [57], when an electromagnetic wave was transmitted through a medium, its absorption property depends on many factors, such as a permittivity, permeability, sample thickness, specific surface area, and the frequency wave. The efficiency of the absorber is linked to the amount of the charge and its degree of the dispersion in the composite. Theoretically, the microwave reflection coefficient RC (dB) [58,59] is calculated from the relative permeability and permittivity at the given frequency and absorber thickness. In a single layered absorber, the electromagnetic wave absorbing property can be evaluated by the following equation [60–62]:

$$Z = Z_0 \cdot \sqrt{\left(\frac{\mu_r}{\varepsilon_r}\right)} \tanh\left(\left(j\frac{2\pi}{c}\right) \sqrt{\mu_r \cdot \varepsilon_r} \cdot f \cdot d\right) \quad (1)$$

$$\text{RC (dB)} = 20 \log \left| \frac{Z - Z_0}{Z + Z_0} \right| \quad (2)$$

where  $\mu_r = \mu'_r - j\mu''_r$  and  $\varepsilon_r = \varepsilon'_r - j\varepsilon''_r$  are the complex magnetic permeability and permittivity of the absorbing media. RC (dB) is the microwave reflection coefficient,  $Z$ , the normalized input impedance at air absorber interface and  $Z_0 = 377 \Omega$  the impedance of free space,  $f$  the frequency of incident wave,  $d$  the absorption layer thickness and  $c$  the velocity of light.

A perfect absorber is given when  $Z = Z_0$ . It can be explained that the relative permittivity and relative permeability should be close to each other. The ideal condition of no reflective wave on surface is  $\mu_r = \varepsilon_r$  indicating the full absorption of microwave [63].

Experimentally, the electromagnetic wave absorbing samples are prepared by molding and curing the mixture of PANI/epoxy composites and PANI/Fe<sub>3</sub>O<sub>4</sub>/epoxy resin hybrid composites at different thickness and amount of fillers. The wave guide is fitted with the sample backed by a metal short as shown in Fig. 5.

The wave absorption property can be deduced from the measurement of the reflection coefficient RC ( $S_{11}$ ) given by the network analyzer:

$$\text{RC} = 20 \log(S_{11}) \quad (3)$$

The dip in RC indicates the occurrences of absorption or minimal reflection of microwave power. The intensity and frequency at the minimum RC are linked to the electromagnetic properties and thickness of samples [64]. Fig. 6 presents the composite frequency dependence of reflection coefficient at different rates of loading fillers and different thicknesses. Composites based on hybrid polyaniline/magnetite/epoxy resin composites have a more obvious effect on microwave absorbing properties than composite without magnetite. Dielectric composites based on PANI/epoxy resin show a reflection coefficient increased with loading of PANI in matrix. It revealed at 18 GHz, a value of  $-3$  dB and  $-11$  dB at 10 and 20% of PANI. These composites have a values of 5, 8.5, of  $\varepsilon'$  and 0.05 and 0.16 of  $\tan(\delta)_\varepsilon$  respectively. However, hybrid EMAMs based on polyaniline/magnetite/epoxy resin with a thickness around 1 mm at different amounts of PANI and Fe<sub>3</sub>O<sub>4</sub> show a minimum reflection coefficient at different frequency as it is presented in Fig. 6b.

Hybrid composites of 15% of PANI with 5, 10, 15, 20 and 25% of magnetite indicate at frequencies of 17.47, 15.38, 14.03, and 14.85 GHz minimum reflection coefficient values of  $-14.33$ ,  $-42.25$ ,  $-42.28$ , and  $-37.33$  dB respectively. However, composite of 20% of PANI without magnetite, gives a value of  $-11$  dB at 18 GHz. Thus, all of composites indicate a value of 90–99.99% of microwave absorption energy at the indicated frequency. These results obviously demonstrate that the intensity and the frequency

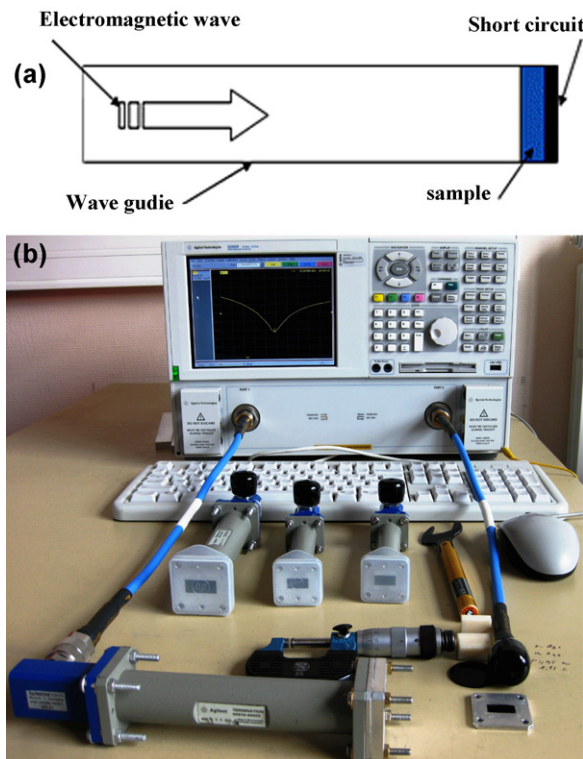


Fig. 5. Reflection coefficient measurements mean (a) and Agilent E8362B Vector Network Analyzer with microwave probe setup for scattering parameters measurements (b).

of the microwave energy absorption for the composite also depend on the rate of the polyaniline and magnetite content in the matrix. Thus, microwave absorption properties of composite are improved by the dielectric and magnetic losses when the weight fraction of Fe<sub>3</sub>O<sub>4</sub> increases. Zou et al. observed that for 1.9 mm of thickness and 70% of Fe<sub>3</sub>O<sub>4</sub>, that the optimal reflection coefficient was  $-42.7$  dB [65]. In our case, the optimum of 15% of PANI and 10% of Fe<sub>3</sub>O<sub>4</sub> leads to  $-42$  dB with a thickness of 1 mm.

The reflection coefficient at different thickness of composites with 15% of PANI and 10% of Fe<sub>3</sub>O<sub>4</sub> which has electromagnetic parameters of 10, 1.2, 0.2 and 0.15 of  $\varepsilon'$ ,  $\mu'$ ,  $\tan(\delta)_\varepsilon$  and  $\tan(\delta)_\mu$  respectively is presented in Fig. 6c. It is found that reflection coefficient depends sensitively on the thickness of the absorber and the dip shifts towards a lower frequency as the thickness of the absorber increases. The increase of the thickness of the sample leads to a higher microwave absorption. It is revealed that, at thicknesses of 1, 1.5, 2.5, 3 and 3.5 mm, the minimum reflection coefficient indicated a values of  $-41.35$ ,  $-38.28$ ,  $-37.28$ ,  $-37.64$  and  $-39.49$  dB at 16.3, 16.06, 15.52, 14.97, and 14.47 GHz respectively.

The calculated absorption spectra for composite based on PANI (15%)/Fe<sub>3</sub>O<sub>4</sub> (10%) epoxy resin have been compared with measured spectra in Fig. 6d. The shapes of both experimental and theoretically calculated spectra are similar. The calculated matching thickness of 2.25 mm for the minimum reflection coefficient is in good agreement with experimental values of 1.47 mm. However, the measured curve does not fit exactly on the theoretical curve. This difference in the measured and the calculated values of reflection coefficient may be further attributed to the surface irregularity of the absorber sample, gap between the sample and wave-guide dimensions, air gap between sample and metal short circuit [66–68]. Different kinds of magnetic fillers are generally used in composite absorbers; but their permeability drastically reduces at high frequencies [69]. However, if the filler is made of ferroelectric and dielectric materials, permeability will remain



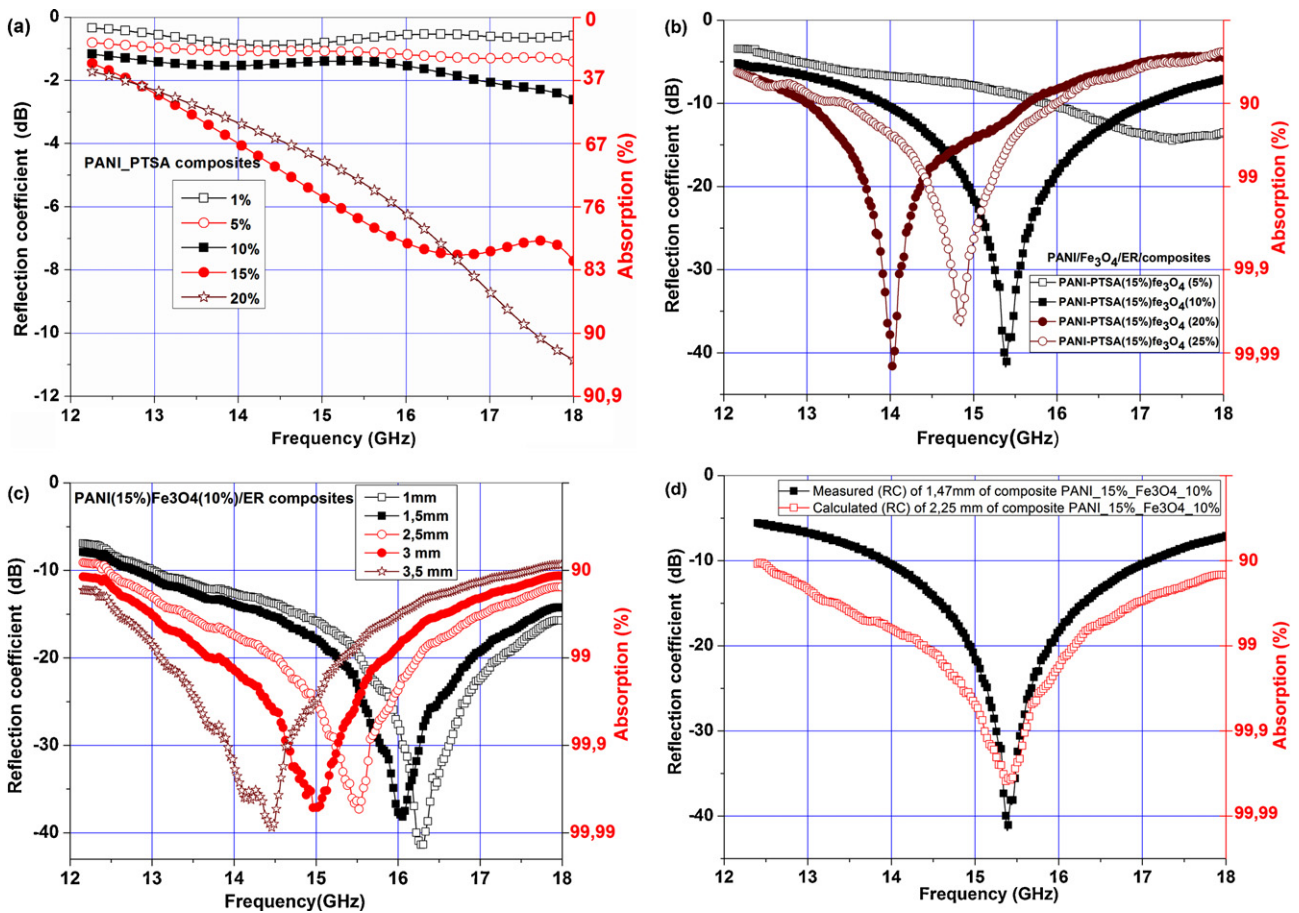


**Fig. 6.** The composites frequency dependence of reflection coefficient at different filler's amount: PANI-PTSA/epoxy resin composites (a), PANI-PTSA/Fe<sub>3</sub>O<sub>4</sub>/epoxy resin hybrid composites (b), PANI-PTSA (15%)/Fe<sub>3</sub>O<sub>4</sub> (10%)/epoxy resin hybrid composites at different thickness (c) and the comparison of measured and calculated reflection coefficient for PANI-PTSA (15%)/Fe<sub>3</sub>O<sub>4</sub> (10%)/epoxy resin hybrid composite (d).

constant throughout the frequency range and their larger propagation constant enables wave absorber to be made thinner. In medium level conductivity materials, a large part of energy radiation is absorbed in the material and transformed into heat; whereas in metallic materials, the radiation is fully reflected. Microwave absorption is caused by the interaction between electric dipole or magnetic dipole in the material and the electromagnetic field. When the conductivity reaches a determinate value, the material with high permeability has high microwave absorption. As mentioned above, materials with higher  $\tan \delta$  are considered lossy materials that indicate strong absorption.

#### 4. Conclusion

Hybrid electromagnetic wave absorbing composites containing polyaniline were successfully prepared and investigated. XRD patterns confirmed the semi-crystallinity of the PANI-doped PTSA and a high crystalline phase of magnetite as shown by the SEM micrographs. The combination of the PANI and magnetic fillers to elaborate a high performance microwave absorbers materials can contribute to reduce the thickness of the materials. The incorporation of Fe<sub>3</sub>O<sub>4</sub> particles leads to high interfacial polarization. The microwave absorption depends on the thickness of the shield and the type and amount of the filler that modify the material electromagnetic properties. Composite made of 20% of PANI showed -11 dB at 18 GHz of reflection coefficient. However a composite with a thickness around 1 mm containing 15% of PANI and 10% of Fe<sub>3</sub>O<sub>4</sub> leads to a minimum coefficient reflection, about of -42 dB,

more than 99.99% of the microwave absorption. These composites with different thicknesses indicate a high value of energy attenuation in this frequency range. These composite materials show high microwave absorption in Ku band and then are promising for technological applications. These results encourage further development of multilayered absorbers for broadband applications.

#### Acknowledgments

The authors would like to express grateful acknowledgment to all researchers of E.M.P, Algeria and Département Chimie – Environnement, at Ecole des Mines de Douai, France, for their experimental assistance and discussions.

#### References

- [1] F. Nanni, P. Travaglia, M. Valentini, *Composites Science and Technology* 69 (2009) 485–490.
- [2] Y. Liu, Z. Zhang, S. Xiao, C. Qiang, L. Tian, J. Xu, *Applied Surface Science* 257 (2011) 7678–7683.
- [3] J.-H. Oh, K.-S. Oh, C.-G. Kim, C.-S. Hong, *Composites Part B: Engineering* 35 (2004) 49–56.
- [4] D. Micheli, C. Apollo, R. Pastore, et al., *IEEE Transactions on Electromagnetic Compatibility* 54 (2012) 60–69.
- [5] S. Ni, X. Wang, G. Zhou, F. Yang, J. Wang, D. He, *Journal of Alloys and Compounds* 489 (2010) 252–256.
- [6] E.T. Thostenson, T.W. Chou, *Composites Part A: Applied Science and Manufacturing* 30 (1999) 1055–1071.
- [7] D.R.J. White, *A Handbook on Shielding Design Methodology and Procedures*, 1986.
- [8] L.A. Ramajo, A.A. Cristobal, P.M. Botta, J.M. Porto Lopez, M.M. Reboredo, M.S. Castro, *Composites Part A: Applied Science and Manufacturing* 40 (2009) 388–393.

- [9] S.M. Abbas, M. Chandra, A. Verma, R. Chatterjee, T.C. Goel, *Composites Part A: Applied Science and Manufacturing* 37 (2006) 2148–2154.
- [10] D.A. Makeiff, T. Huber, *Synthetic Metals* 156 (2006) 497–505.
- [11] S.K. Dhawan, K. Singh, A.K. Bakhshi, A. Ohlan, *Synthetic Metals* 159 (2009) 2259–2262.
- [12] P. Chandrasekhar, K. Naishadham, *Synthetic Metals* 105 (1999) 115–120.
- [13] N.H. Hoang, J.L. Wojkiewicz, J.L. Miane, R.S. Biscarro, *Polymers for Advanced Technologies* 18 (2007) 257–262.
- [14] K.K. Satheesh Kumar, S. Geetha, D.C. Trivedi, *Current Applied Physics* 5 (2005) 603–608.
- [15] C.Y. Lee, H.G. Song, K.S. Jang, E.J. Oh, A.J. Epstein, J. Joo, *Synthetic Metals* 102 (1999) 1346–1349.
- [16] T. Makela, S. Pienimaa, T. Taka, S. Jussila, H. Isotalo, *Synthetic Metals* 85 (1997) 1335–1336.
- [17] N. Gandhi, K. Singh, A. Ohlan, D.P. Singh, S.K. Dhawan, *Composites Science and Technology* 71 (2011) 1754–1760.
- [18] L. de Castro Folgueras, M.A. Alves, M.C. Rezende, *Materials Research* 11 (2008) 245–249.
- [19] G. Tong, W. Wu, J. Guan, H. Qian, J. Yuan, W. Li, *Journal of Alloys and Compounds* 509 (2011) 4320–4326.
- [20] Y. Li, G. Chen, Q. Li, G. Qiu, X. Liu, *Journal of Alloys and Compounds* 509 (2011) 4104–4107.
- [21] B. Belaabed, J.L. Wojkiewicz, S. Lamouri, N. El Kamchi, N. Redon, *Polymers for Advanced Technologies* (2011), doi:10.1002/pat.2029.
- [22] M. Akatsuka, Y. Takezawa, S. Amagi, *Polymer* 42 (2001) 3003–3007.
- [23] S.W. Phang, M. Tadokoro, J. Watanabe, N. Kuramoto, *Synthetic Metals* 158 (2008) 251–258.
- [24] Y. Yang, S. Qi, J. Wang, *Journal of Alloys and Compounds* 520 (2012) 114–121.
- [25] S. Yang, K. Lozano, A. Lomeli, H.D. Foltz, R. Jones, *Composites Part A: Applied Science and Manufacturing* 36 (2005) 691–697.
- [26] Z. Wang, H. Bi, J. Liu, T. Sun, X. Wu, *Journal of Magnetism and Magnetic Materials* 320 (2008) 2132–2139.
- [27] S.H. Hosseini, S.H. Mohseni, A. Asadnia, H. Kerdari, *Journal of Alloys and Compounds* 509 (2011) 4682–4687.
- [28] B. Belaabed, S. Lamouri, N. Naar, P. Bourson, S. Ould Saad Hamady, *Polymer Journal* 42 (2010) 546–554.
- [29] B. Belaabed, S. Lamouri, J.L. Wojkiewicz, *Polymer Journal* 43 (2011) 683–691.
- [30] Y. Wang, M.N. Afsat, K. Grignon, *IEEE International Symposium on Antennas and Propagation Society*, Columbus, OH, 2003, pp. 619–622.
- [31] N.N. Al-Moayed, M.N. Afsar, U.A. Khan, S. McCooley, M. Obol, *IEEE Transactions on Magnetics* 44 (2008) 1768–1772.
- [32] V.N. Prigodin, A.J. Epstein, *Synthetic Metals* 125 (2001) 43–53.
- [33] J. Wang, J. Wang, Z. Yang, Z. Wang, F. Zhang, S. Wang, *Reactive and Functional Polymers* 68 (2008) 1435–1440.
- [34] Y.-G. Han, T. Kusunose, T. Sekino, *Synthetic Metals* 159 (2009) 123–131.
- [35] P.M. Beadle, Y.F. Nicolau, E. Banka, P. Rannou, D. Djurado, *Synthetic Metals* 95 (1998) 29–45.
- [36] M.E. Jozefowicz, A.J. Epstein, J.P. Pouget, J.G. Masters, A. Ray, Y. Sun, X. Tang, A.G. MacDiarmid, *Synthetic Metals* 41 (1991) 723–726.
- [37] J.E. Fischer, X. Tang, E.M. Scherr, V.B. Cajipe, A.G. MacDiarmid, *Synthetic Metals* 41 (1991) 661–664.
- [38] S. Bhadra, D. Khastgir, *Polymer Testing* 27 (2008) 851–857.
- [39] J. Joo, Y.C. Chung, H.G. Song, J.S. Baeck, W.P. Lee, A.J. Epstein, A.G. MacDiarmid, S.K. Jeong, E.J. Oh, *Synthetic Metals* 84 (1997) 739–740.
- [40] M. Zilberman, G.I. Titelman, A. Siegmann, Y. Haba, M. Narkis, D. Alperstein, *Journal of Applied Polymer Science* 66 (1997) 243–253.
- [41] Z. Zou, A.G. Xuan, Z.G. Yan, Y.X. Wu, N. Li, *Chemical Engineering Science* 65 (2010) 160–164.
- [42] H. Guo, H. Zhu, H. Lin, J. Zhang, *Materials Letters* 62 (2008) 2196–2199.
- [43] K. Jia, R. Zhao, J. Zhong, X. Liu, *Journal of Magnetism and Magnetic Materials* 322 (2010) 2167–2171.
- [44] K.C. Pitman, M.W. Lindley, D. Simkin, J.F. Cooper, *IEEE Proceedings-F* 38 (1991) 223–228.
- [45] K. Singh, A. Ohlan, A.K. Bakhshi, S.K. Dhawan, *Materials Chemistry and Physics* 119 (2010) 201–207.
- [46] C. Hou, T. Li, T. Zhao, W. Zhang, Y. Cheng, *Materials & Design* 33 (2012) 413–418.
- [47] Y. Yao, H. Jiang, J. Wu, D. Gu, L. Shen, *Procedia Engineering* 27 (2012) 664–670.
- [48] S.B. Kumar, H. Hohn, R. Joseph, M. Hajian, L.P. Ligthart, K.T. Mathew, *Journal of the European Ceramic Society* 21 (2001) 2677–2680.
- [49] X.L. Dong, X.F. Zhang, H. Huang, F. Zuo, *Applied Physics Letters* 92 (2008) 013127.
- [50] Z. Li, Y. Deng, B. Shen, W. Hu, *Materials Science and Engineering B* 164 (2009) 112–115.
- [51] K.H. Wu, T.H. Ting, G.P. Wang, C.C. Yang, C.W. Tsai, *Synthetic Metals* 158 (2008) 688–694.
- [52] A.B. Afzal, M.J. Akhtar, M. Nadeem, M.M. Hassan, *Current Applied Physics* 10 (2010) 601–606.
- [53] J.D. Sudha, S. Sivakala, R. Prasanth, V.L. Reena, P. Radhakrishnan Nair, *Composites Science and Technology* 69 (2009) 358–364.
- [54] P. Tsotra, K. Friedrich, *Journal of Materials Science* 40 (2005) 4415–4417.
- [55] C. Reis Martins, R. Faez, M. Cerqueira Rezende, M.-A. Paoli, *Polymer Bulletin* 51 (2004) 321–326.
- [56] Z. He, Y. Fang, X. Wang, H. Pang, *Synthetic Metals* 161 (2011) 420–425.
- [57] E. Michielssen, J.-M. Sajer, S. Ranjithan, R. Mittra, *IEEE Transactions on Microwave Theory and Techniques* 41 (1993) 024–1031.
- [58] D. Micheli, C. Apollo, R. Pastore, M. Marchetti, *Composites Science and Technology* 70 (2010) 400–409.
- [59] D. Micheli, C. Apollo, R. Pastore, R. Bueno Morles, S. Laurenzi, M. Marchetti, *Acta Astronautica* 69 (2011) 747–757.
- [60] Y. Naito, K. Suetake, *IEEE Transactions on Microwave Theory and Techniques* 19 (1971) 65–72.
- [61] Z. Jun, T. Peng, W. Sen, X. Jincheng, *Applied Surface Science* 255 (2009) 4916–4920.
- [62] D. Micheli, R. Pastore, C. Apollo, M. Marchetti, G. Gradoni, V. Mariani Primiani, F. Moglie, *IEEE Transactions on Microwave Theory and Techniques* 59 (2011).
- [63] W.-p. Li, L.-q. Zhu, J. Gu, H.-c. Liu, *Composites Part B: Engineering* 42 (2011) 626–630.
- [64] S.W. Phang, R. Daik, M.H. Abdullah, *Thin Solid Films* 477 (2005) 125–130.
- [65] S.M. Abba, R. Chatterjee, A.K. Dixit, A.V.R. Kumar, T.C. Goel, *Journal of Applied Physics* 101 (2007) 074108.
- [66] P. Singh, V.K. Babbar, A. Razdan, S.L. Srivastava, T.C. Goel, *Materials Science and Engineering B* 78 (2000) 70–74.
- [67] S.M. Abbas, A.K. Dixit, R. Chatterjee, T.C. Goel, *Materials Science and Engineering B* 123 (2005) 167–171.
- [68] P. Singh, V.K. Babbar, A. Razdan, S.L. Srivastava, R.K. Puri, *Materials Science and Engineering B* 67 (1999) 132–138.
- [69] I. Kong, S. Hj Ahmad, M. Hj Abdullah, D. Hui, A. Nazlim Yusoff, D. Puryanti, *Journal of Magnetism and Magnetic Materials* 322 (2010) 3401–3409.